Article

Deformation Characteristics of Combined Heavy Metals-Contaminated Soil Treated with nZVI through the Modified Slurry Consolidation Method

Chen Fan [1], Yongzhan Chen [1],*, Qinxi Dong [1],[2],*, Jing Wei [1] and Meng Zou [1]

[1]   School of Civil Engineering and Architecture, Hainan University, Haikou 570228, China;
      21220856000147@hainanu.edu.cn (C.F.)
[2]   Development Report of Key Laboratory of Equipment Safety and Intelligent Technology for Guangzhou Rail
      Transit System, Guangzhou 511300, China
*   Correspondence: yongzhan_chen@hainanu.edu.cn (Y.C.); dongqinxi@hainanu.edu.cn (Q.D.)

Abstract: Nanoscale zero-valent iron (nZVI) has been widely applied to remediate heavy metal-contaminated soils and water. Its in situ treatment of combined heavy metal contaminated soil, followed by backfilling or other sustainable reutilizations, attracted attention to the treated soil's deformation characteristics. In this study, soil samples were prepared using the modified slurry consolidation method to simulate the natural settling of backfilled soil and optimize the reactivity between nZVI and contaminants in soil. The deformation characteristics of natural soil, contaminated soil, and soil treated with varying dosages of nZVI (0.2%, 0.5%, 1%, 2%, and 5%) were investigated. Moreover, the plasticity indexes and particle-size distribution of the samples were examined through Atterberg limits and laser-diffraction particle-size analysis. After a 4 d slurry consolidation process, a typical result indicated the immobilization efficiency of all three heavy metal ions achieved over 90% with 2% nZVI. The presence of three heavy metal ions decreased the Atterberg limits and increased the compression index, permeability, and consolidation coefficient of the soil. Conversely, the introduction of nZVI increased plasticity and resulted in higher permeability, stable secondary consolidation, and less swell. Microscopically, with an increase in the dosage of nZVI, the soil aggregates transformed from a weak chemical bond with insoluble precipitates/iron oxides to larger aggregates consisting of nZVI/-soil aggregates, thereby enhancing the soil skeleton. This study shows improved permeability and deformation characteristics in nZVI-treated combined heavy metal-contaminated soil, offering valuable insights for practical nanomaterials' in-situ treatment in engineering applications.

Keywords: combined heavy metals-contaminated soil; nanoscale zero-valent iron (nZVI); deformation characteristics; aggregation; slurry consolidation method

1. Introduction

Contaminated soil poses a significant threat to the sustainable utilization of land resources and gives rise to severe ecological concerns [1,2]. Heavy metal contaminants have garnered widespread attention from both the public and the academic community due to their high toxicity, strong mobility, and persistent presence [3–5]. Heavy metal ions, such as Pb(II), Cd(II), Ni(II), Zn(II), and others in subwater and soil, pose a grave risk to the health of living organisms through biological chain enrichment. It is worth noting that these harms include not only human organ tissues and the nervous system but also increasing the risk of cancer [6–11]. In practice, soil samples affected by contamination often exhibit the simultaneous presence of multiple heavy metal ions, such as approximately 2.5 million heavy metals and organics contaminated sites in Europe [12], more than 235,000 in-/organic locations in the US [13], and 16.1% of the country's total land combined contaminated area in China [14]. Therefore, the issue of combined heavy metals contaminated soil urgently

requires resolution for the sustainability of soil and sites, particularly in both environmental and geotechnical aspects.

Previous studies have explored the treatment of contamination in soil and contaminated soil in the past few decades and treatment attempts included physical, bioremediation, chemical, and comprehensive multimethod ways. Many studies have confirmed the potential of nanomaterials for chemical remediation methods to rapidly decrease the concentration of heavy metal ions, and they are excellent and environmentally friendly in both soil and water. Among these nanomaterials, nano zero-valent iron (nZVI) has gained significant attention due to its high reactivity, reductive capabilities, and nontoxicity. It can efficiently degrade single, double, or even combined complex heavy metal ions, making it a prominent focus of nanomaterial remediation research in recent years. When used in appropriate quantities, nZVI can achieve degradation efficiencies of over 99% for Pb(II) [15] or Ni(II) [16] in a short time. In combined contaminant solutions, it has been shown to achieve degradation efficiencies of over 92% for Cu, Ag, Pb, Cr, and Zn. When dealing with Ni(II)-contaminated soil, nZVI achieved an 85% degradation efficiency [17]. In the case of binary-contaminated soil (Pb(II) and Zn(II)), nZVI exhibited an 80% immobilization efficiency [18]. In a combined contaminated soil, nZVI has demonstrated degradation efficiencies exceeding 92% for Cd(II), Cu(II), Ni(II), and Pb(II) [19]. Numerous studies have affirmed the potential of nanomaterials within chemical remediation methods for rapidly reducing the concentration of heavy metal ions in soil. For instance, notable soil-remediation examples included the reduction in 72% Pb(II) and 90% Cd(II) by nano-hydroxyapatite [20], 100% removal of Cu(II) and Pb(II) by a modified nano-clay [21], 97% degradation efficiency of Cd(II) and Zn(II) by a combination containing nano-iron [22], and over 88% of Ni(II) in a short period by nano-calcium silicate [23]. With the high efficiency of combined contaminants' remediation, it would offer the possibility of sustainable reuse of contaminated sites. Therefore, using the nanomaterial—nZVI—for remediating heavy metal-contaminated soil is, thus, a feasible and preferred approach, while the multiple reaction mechanisms among nZVI–water–contaminants–soil cannot be ignored.

The mechanisms for degrading heavy metals with nZVI involved reduction, adsorption, precipitation, and coprecipitation, classified as both chemical and physical processes with soil [24,25]. Redox reactions can be explained using standard electrode potentials (E^0). Heavy metal ions (e.g., -0.809 V Cd(II) and -0.763 V Zn(II)) with E^0 values less negative or equivalent to Fe^0 (i.e., -0.440 V) are primarily removed through adsorption onto the iron hydroxide shell. Metal ions with significantly more positive E^0 values than Fe^0 (e.g., $+0.248$ V As(III), $+0.342$ V Cu(II), $+0.797$ V Hg(II), and $+1.232$ V Cr(VI),) are mainly eliminated through reduction and precipitation. Metal ions with moderately positive E^0 values compared to Fe^0 (e.g., -0.126 V Pb(II) and -0.246 V Ni(II)) can be degraded through both reduction and adsorption mechanisms [26,27]. Specific heavy metal ions, like Pb(II), Cd(II), and Cu(II), can react with ferrous ions that are released, leading to the formation of insoluble metal compounds immobilized in the soil or water. In addition to its high reactivity and reducibility, nZVI and its products have strong aggregative tendencies, magnetic properties, and an exceptionally large surface area [28–30]. After the transformation of metallic iron at the nanoscale, the particles tend to aggregate due to nanoscale forces. Simultaneously, during the process of the "physical process" of nZVI in soil, they precipitate and adsorb onto soil particles. Due to the scale similarity between nanomaterial aggregates and soil particles, the effect of this microphysical interaction on macroscopic geotechnical properties is of interest. Thus, it necessitates a comprehensive evaluation of engineering safety at the remediation site by nZVI, in which the approach with an optimized reaction environment for nZVI in soil could lay the groundwork for further explorations.

The preliminary research results indicated few studies on the geotechnical properties of soil treated with nZVI, while it can be discerned that nZVI will have a noticeable effect on the deformation of soil. Deformation parameters (e.g., compression index, swelling index, creep/consolidation coefficient, etc.) represent an important criterion for engineering safety assessments. The introduction of nZVI has been found to alter the microstructure

of contaminated soil, subsequently impacting its deformation characteristics and then affecting the reuse of treated sites. When an appropriate or excessive amount of nZVI is used for degrading Pb(II) in the soil, the products generated tend to precipitate on the surfaces of soil particles, forming large aggregates and dense connection structures, resulting in reduced soil porosity and expansion index [31]. Soil permeability can also serve as a measure of deformation characteristics [32]. Research has shown that an excess of nZVI can lead to the formation of larger aggregates in the soil, subsequently blocking pores and causing a decrease in soil permeability [33], which reveals a reduction in the consolidation coefficient and an enhancement in soil compressibility. However, different application conditions will lead to different experimental results, which need to be analyzed specifically. As for the insufficient information about nZVI treatment in soil, it becomes evident that the impact of nanomaterials on the deformation and permeability of contaminated soil can vary significantly, referencing other cases of nanomaterial treatment. For instance, the addition of nano-magnesium dioxide to Pb(II) and Zn(II) co-contaminated soil leads to a reduction in the soil's compression index and hydraulic conductivity [34,35]. Furthermore, some studies have indicated that the presence of nano-clay alters the cation exchange capacity (CEC) and specific surface area (SSA) within the system, subsequently increasing permeability and settling in soils with high copper concentrations, up to 30 cmol/kg nitric acid [36]. These findings highlight the complexity and diversity of macroscopic property changes triggered by the introduction of nanomaterials into contaminated soil. It is important to note that previous research results indicated a pronounced aggregation effect of nanomaterials in the soil, which subsequently affected changes in deformation properties [37–39]. From the aspect of geotechnical improvement, the greatest value of a treated site is sustainable use, among which the most critical issues are engineering safety issues, such as deformation characteristics. However, limited research has been done on the deformation characteristics and microstructure of combined heavy metal-contaminated soil after nZVI treatment. Consequently, close attention is required to focus the changes in deformation properties induced by nZVI into combined contaminated soil.

This study employs varying dosages of nZVI to treat Pb(II) (reduction), Zn(II) (precipitation), and Ni(II) (adsorption) combined in contaminated soil, investigating the deformation characteristics and microstructure of the treated soil. The objective is to explore the deformation characteristics and mechanisms underlying the role of nZVI in combined contaminated soil with heavy metals and understand the reasons behind the changes in microscopic ways induced by nZVI. All the samples were prepared by the modified slurry consolidation method to make sure the additions could react efficiently with heavy metals and soil particles, through which it could simulate the process of reusing disposed of soil backfill in the project. Specifically, multistage loading and unloading oedometer tests were employed to study the deformation properties of natural, contaminated, and treated soils. Before that, the Toxicity Characteristic Leaching Procedure (TCLP) was conducted for the immobilization efficiency of each heavy metal ion. Additionally, the plasticity and particle-size distribution of different samples were analyzed using Atterberg limits analysis and laser-diffraction particle-size analysis, respectively, to interpret the impact of composite heavy metal ions and nZVI on the geotechnical properties of soils from a microscopic perspective. The efficient, safe, and sustainable solutions of the advanced nanomaterial could be an indicator for future nanomaterials research in soil, contributing to the sustainable research development of Nano-Geotechnical Engineering.

2. Materials and Methods

2.1. Materials

2.1.1. Soil

The experimental sediment soil was collected from the city lake in Haikou. X-ray diffraction (XRD) analysis results (Figure 1) showed that the main minerals in the soil were quartz, franklinite, and halite. The liquid limit of the soil was 97.0%, and the plastic limit was 35.0%, according to ASTM D4318-17 [40]. The optimal moisture content was

determined to be 22.0%, and the maximum dry density was determined to be 1.75 g/cm^3, using the compaction method according to ASTM D698-12 [41]. Laser particle-size analyzer results indicated that the sediment contained 18.0% clay, 80.0% silt, and 2.0% sand. Based on the Unified Soil Classification System (USCS, ASTM D2487-17 [42]), the matrix soil was classified as high plasticity silt (MH).
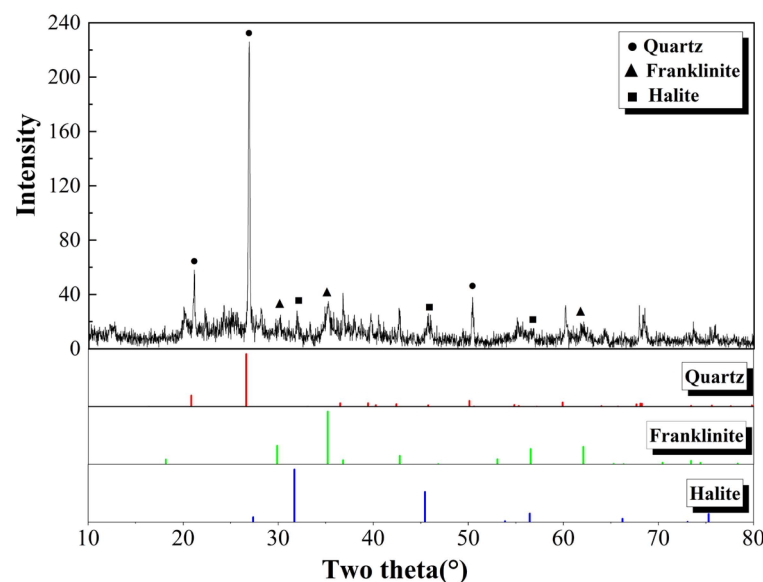
Figure 1. XRD analysis of experimental sediment soil.

2.1.2. Contaminants and nZVI

The contaminants used in the experiment included $Pb(NO_3)_2$, $Ni(NO_3)_2$, and $Zn(NO_3)_2$. These chemicals were analytical grade (AR) and supplied by Guanghua Technology Corp (Guangdong, China). These contaminants were selected by considering the mechanism of heavy metal contamination by nZVI treatment, such as reduction—Pb(II), precipitation—Zn(II), and adsorption—Ni(II). Nitrate is inert and has a facilitating effect in nZVI treatment while avoiding the precipitation of anions with contaminating cations.

The commercial nZVI used in the experiment was prepared by a plasma sputtering method and provided by Xiang-Tian Corp (Shanghai, China). The particles have an average diameter of 50 nm and a purity of 99.9%, and the specific surface area was 30.58 m^2/g. They were supplied by Xiang-Tian Corp.

2.1.3. Toxic Leaching Reagent

The leaching reagents used in the experiment include AR chemicals, such as solid sodium hydroxide, concentrated nitric acid, and glacial acetic acid, which were supplied by Xilong Technology Corp (Guangdong, China).

2.2. Methods

2.2.1. Preparation of Soil Samples

The soil samples used in the experiment were prepared by the modified slurry consolidation method; it has been proved that the process could simulate the settlement of soil under backfill and consolidation conditions [37]. Specifically, the collected soil, after the removal of branches and stones, was made into a slurry and sieved through 1 mm in its natural state. Then, the sieved slurry was adjusted to twice the liquid limit, ensuring homogenization like a solution state. Simultaneously, the increase in moisture content enhanced the fluidity and dispersibility of the slurry, facilitating the migration of nanoparticles. By this, the effective interaction among the particles (soil particles, nZVI, and heavy metal ions) could be improved. Three heavy metal contaminants were individually weighed in 200 mg/kg (dry soil weight) of their ion mass and dissolved in 1 L of deionized water.

Once the contaminants had fully dissolved, they were added to the prepared slurry; then, the total concentration of heavy metal ions was 600 mg/kg (i.e., Pb(II) 200 mg/kg, Zn(II) 200 mg/kg, and Ni(II) 200 mg/kg). The mixture was continuously stirred and then allowed to settle for 48 h to ensure adsorption equilibrium, chemical reactions, microbial effects, and a more uniform state in or with the soil. Various dosages, such as 0.2%, 0.5%, 1%, 2%, and 5% (dry soil weight), of nZVI particles were added into the contaminated slurry under ultrasonic and stirring conditions. After following the recommended mixing reaction time of 10 min, it could achieve a full dispersion and reactions of nZVI in the soil slurry, which has been proven by the literature [31,37,43,44]. Then, the treated slurry was transferred to a double-drainage tank for a preconsolidation process with effective vertical stress of approximately 100 kPa, which was confirmed through Casagrande's method in trial oedometer tests. The 1-D consolidation process was considered to be ended once the incremental vertical strain was less than 1%/d. Samples for the Oedometer test were obtained using a standard ring with a diameter of 50 mm and a height of 20 mm, while the remaining soil was used for further experiments (as suggested in ASTM D2435/D2435M-1 [45]). Furthermore, the samples prepared have been proven to be fully saturated.

2.2.2. Toxicity Characteristic Leaching Procedure (TCLP)

According to the instruction (EPA method 1311 2015 [46]), the pH values of the water leached from soil samples after the process of the slurry-mixing procedure consistently exceeded 5. Consequently, a 1# extractant was utilized to extract free heavy metal ions from the soil. Specifically, 20 g of the soil sample were oven-dried at 105 °C for 24 h. Then, the dried soil was smashed and sieved through 1 mm. A solution comprising 0.57 mL of glacial acetic acid dissolved in 100 mL of deionized water served as the 1# extractant. Forty mL of the extractant were thoroughly mixed with 2 g of dried soil powder in the extraction bottle. The extraction bottle was then positioned on a rotary shaker (HX-ZD-600A, Huaxi, China) at 23 °C for 18 h. Subsequently, 1 mL of the filtrate underwent a tenfold dilution with 1 M nitric acid (resulting in a dilution solution with a pH of less than 2) before analysis for heavy metal concentrations using inductively coupled plasma optical emission spectroscopy (ICP-OES, Plasma 3000, NCS, China).

Calculate the immobilization efficiency of different heavy metal ions in different soils based on Equation (1) [47,48].

$$I = 1 - \frac{C_f}{C_0} \times 100\% \tag{1}$$

where C_0 means the initial concentration of heavy metals in the soil (103.09 ppm for each heavy metal), and C_f represents the concentration of heavy metals leached out.

2.2.3. Oedometer Tests

The deformation characteristics of saturated soil samples, through the modified slurry-consolidation method, were examined using an Automatic Oedometer (TKA-1, China) in accordance with the ASTM D2435/D2435M-1 [45]. The samples with 20 mm in height and 50 mm in diameter were subjected to consolidation loads in the preconsolidation–compression–unload–reload–compression sequence: 10-50-100-200-400-200-100-200-400-800-1600 kPa, with each load duration of 24 h. Throughout this process, the consolidation ring and the samples were immersed in pure water to ensure and keep a full saturation. Before that, the saturation of extracted samples was double-checked and all were larger than 98%.

The initial void ratio (e_0) and void ratio (e) were determined using Equation (2), where V, V_v, and V_s represented the volume of the sample, the volume of the void, and the volume of particles (Section 12.2 of ASTM D2435/D2435M-11 [45]).

$$\begin{aligned} e_0 &= \frac{V_v}{V_s} = \frac{V - V_s}{V_s} \\ e &= \frac{V_{v1}}{V_s} = \frac{V_1 - V_s}{V_s} \end{aligned} \tag{2}$$

According to Equation (3), the compression index (C_c) was determined using the void ratio at the straight-line section during the compression stage. The swelling index (C_s) was calculated based on the void ratio at 400 kPa and 100 kPa during the rebound stage. And the creep coefficient (C_α) was obtained using the void ratio at 22 to 24 h under each load level.

$$C_C / C_S / C_\alpha = \frac{e_1 - e_2}{\log p_2 - \log p_1} \tag{3}$$

The coefficient of consolidation (C_V) was computed by the time-logarithm method as Equation (4), where T_{50} was 0.197, H_{D50} represented the length of the drainage path at 50% consolidation (cm), and t_{50} meant the time corresponding to 50% consolidation (s).

$$C_V = \frac{T_{50} H_{D50}^2}{t_{50}} \tag{4}$$

The permeability (k) was derived from the coefficient of consolidation by Equation (5), where a and γ_w meant the compression coefficient under a certain load level and the heaviness of water (9.8 kN/m^3).

$$k = \frac{a C_V \gamma_w}{1 + e} \tag{5}$$

2.2.4. Microscopic Characterization

1. XRD analysis

An X-ray diffractometer (DX-2700BH, Haoyuan, China) was used to analyze the composition of nZVI and natural soil powders. Dry powders were placed into the concave groove of a slide, ensuring that the surfaces of the measured powders were approximately 0.1 mm above the slide. The XRD scanning speed was set at 0.05°/min, with a diffraction angle range of 10–80°. The X-ray radiation conditions were set to 40 kV and 40 mA;

2. Atterberg limits

The Atterberg limits were determined through the cone penetrometer method, as prescribed in BS1377:1990. Specifically, the cone penetrometer (LP-100D, Glory Testing, China) was used to measure the cone penetration of the soils at varying moisture contents. The cone used was made of stainless steel, with a length of 35 mm and an angle of 30°. The pretest indicated that the moisture content at a cone penetration of 5 mm was consistent with that determined through the strip rubbing method (ASTM D4318-17 [40]). Therefore, the moisture contents at cone penetrations of 20 mm and 5 mm were determined as the liquid limit (LL) and plastic limit (PL).

3. Particle-size distribution (PSD)

After the slurry consolidation preparation, approximately 0.1 g of the soil sample was dispersed in 30 mL of ultrapure water. The mixture was shaken and then ultrasonically dispersed particle aggregates to meet the requirements. Subsequently, the soil sample was measured for particle size using a Malvern 3000 laser-diffraction particle-size analyzer (Malvern, UK).

3. Results and Discussion

3.1. Immobilization of Heavy Metal Ions

To explore the efficiency of various nZVIs in reacting with combined heavy metal ions within the soil, the time points were selected as reference milestones to occur four days after slurry consolidation. The immobilization efficiency of three heavy metal ions was assessed through the application of the toxicity characteristic leaching procedure (TCLP) and inductively coupled plasma optical emission spectroscopy (ICP-OES). A summary of these findings and the dominant mechanisms are presented in Figure 2.
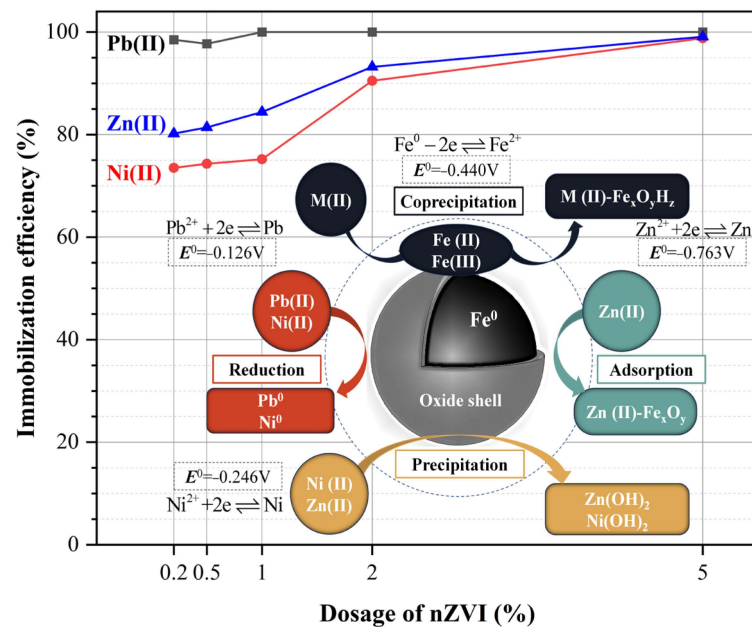
Figure 2. Immobilization efficiency of heavy metals in soil with various dosages of nZVI and its dominant mechanisms.

The results revealed an excellent immobilization efficacy by nZVI when addressing three types of heavy metal contamination ions. Notably, a variation in treatment efficiency is observed across different heavy metal types, with Pb exhibiting the highest efficiency, followed by Zn(II) and Ni(II) (i.e., Pb(II) > Zn(II) > Ni(II)). An excess amount of nZVI (2%) in soil contaminated with combined heavy metal ions was capable of achieving over 90% within just 4 days for Pb(II), Ni(II), and Zn(II). Furthermore, this high efficiency remains stable at 95% or higher for all three heavy metal ions with 5% nZVI. Specifically, at an nZVI dosage of only 0.2%, Pb(II) achieved a 98% efficiency within 4 days, Zn(II) at 80.2%, and Ni(II) at 73.5%, with 0.5%, Pb(II) undergoing complete degradation to approximately 97.5%. The initial efficiency for Zn(II) and Ni(II) increased by 1% and 2%, respectively. At 1%, nZVI achieved an 85% degradation efficiency for Zn(II) within 4 days, which was similar to that observed at 0.2%. Upon reaching 2%, nZVI rapidly attained a degradation efficiency of 90% or higher for all three contaminants in the short term, and it reached above 95% at 5%. In summary, the dosages of nZVI have a significant impact on the degradation efficiency of heavy metal ions in soil contaminated with combined contaminants. nZVI can rapidly immobilize free heavy metal ions in the soil, maintaining stability [15–17]. This finding indicated that nZVI demonstrates exceptional efficiency in the treatment of Pb(II), Zn(II), and Ni(II) within soil systems, while it has a slightly lower reaction efficiency compared to its performance in solution. Simultaneously, a key issue to consider is that, within soil systems, nZVI engages in both chemical processes and physical interactions with water, gases, and soil particles through its unique properties as a nanomaterial. Under conditions where contaminant concentrations are relatively limited with nZVI, the intensity of chemical processes is constrained, leading to a greater proportion of physical interactions with an excess of nZVI [18,19]. In comparing Pb(II), Zn(II), and Ni(II) ions, Pb(II) shows a higher oxidation-reduction potential. These characteristics lead nZVI to preferentially use electron transfer to degrade Pb(II), as Pb(II) ions are more likely to accept electrons from the nZVI surface [49]. During this degradation, hydroxide ions are produced, causing Zn(II) to be a precipitation [50]. Additionally, nZVI only reduces Ni(II) when it is in excess. The iron oxides formed on the thin shell of nZVI during oxidation tend to adsorb Ni(II) [51]. As a result, the effectiveness of nZVI in immobilizing these ions in soil follows the order of Pb(II) > Zn(II) > Ni(II). With the high efficiency of combined contaminants' remediation, it would offer the possibility of sustainable reuse of contaminated sites. It should be noted that the chemical and physical processes within the system, which may be influenced by

the form of heavy metals and reaction products in the soil following different nZVI dosages, could affect the soil's deformation characteristics and microstructure.

3.2. Deformation Analysis

Traditionally, as for heavily contaminated sites, ex situ remediation was regarded as the preferred way to treat and reuse soil from sites. Slurry treatment combined with dehydration and backfill is the widely used approach in current projects, which was considered in our approach. After backfilling, the greatest value of a treated site is sustainable use, among which the most critical issues are engineering safety issues, such as deformation characteristics. When a vertical load is applied to a soil deposit, it results in a decrease in the volume of void space between the soil particles. This reduction in volume leads to an increase in the density of the soil mass, causing settlement.

The section was to conduct one-dimensional consolidation tests on cylindrical soil specimens and analyze the results to determine the soil's compression index (C_c), swelling index (C_s), creep/consolidation coefficient (C_α/C_v), and calculated permeability (k). The compressibility was represented by the relationship between the void ratio and the logarithm of time (Figure 3a). The compression index and swelling index were measures of soil compressibility, calculated as the slope of the linear portion of the curve which is supplied in Figure 3b. Figure 4 provides a summary of the time-strain curves with different nZVIs.
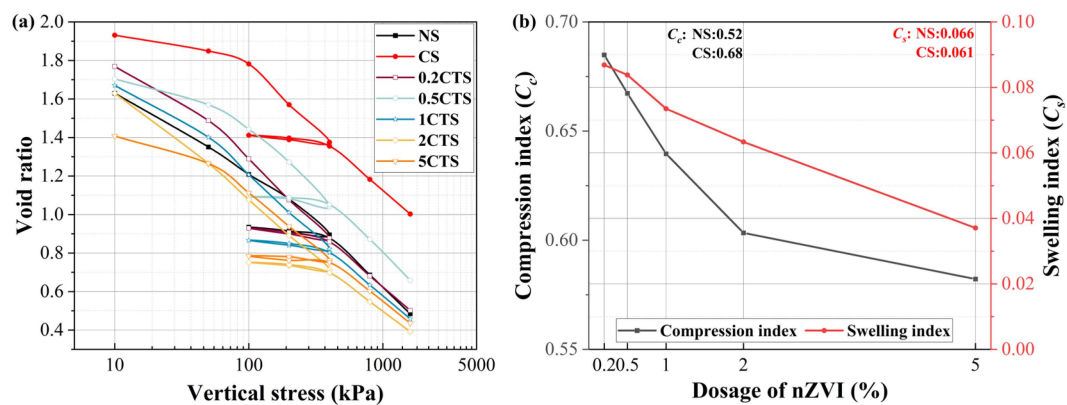
Figure 3. Variations in (**a**) void ratio versus vertical stress curves of samples under different treatments and (**b**) variations in C_c and C_s with different nZVI dosages.

Through the *e*-log*p* curve calculations, it is evident that heavy metal ions had a small influence on the compressibility of the soil with a 10% total settlement and slightly swelling index decrease. The CTS with the higher dosage showed a lower initial void ratio. The 0.2% nZVI enhanced the compressibility of the soil, and the settlement increased by about 10% compared to CS, while the swelling index increased to 0.087. When the nZVI dosage increased to 0.5%, the compression index decreased by 0.017 compared to that of 0.2 CTS, and the swelling index decreased slightly to 0.084. After treatment with 1%, 2%, and 5% nZVI, the compression index further decreased to 0.64, 0.6, and 0.58, respectively. Simultaneously, the swelling index also showed a decreasing trend until reaching 0.037 (over 50% reduction compared to 0.2 CTS). The introduction of heavy metal ions had a limited impact on the compressibility characteristics of the soil, but, due to the increase in cation concentrations in the pore fluid and the decrease in particle spacing, the impact on rebound was significant.
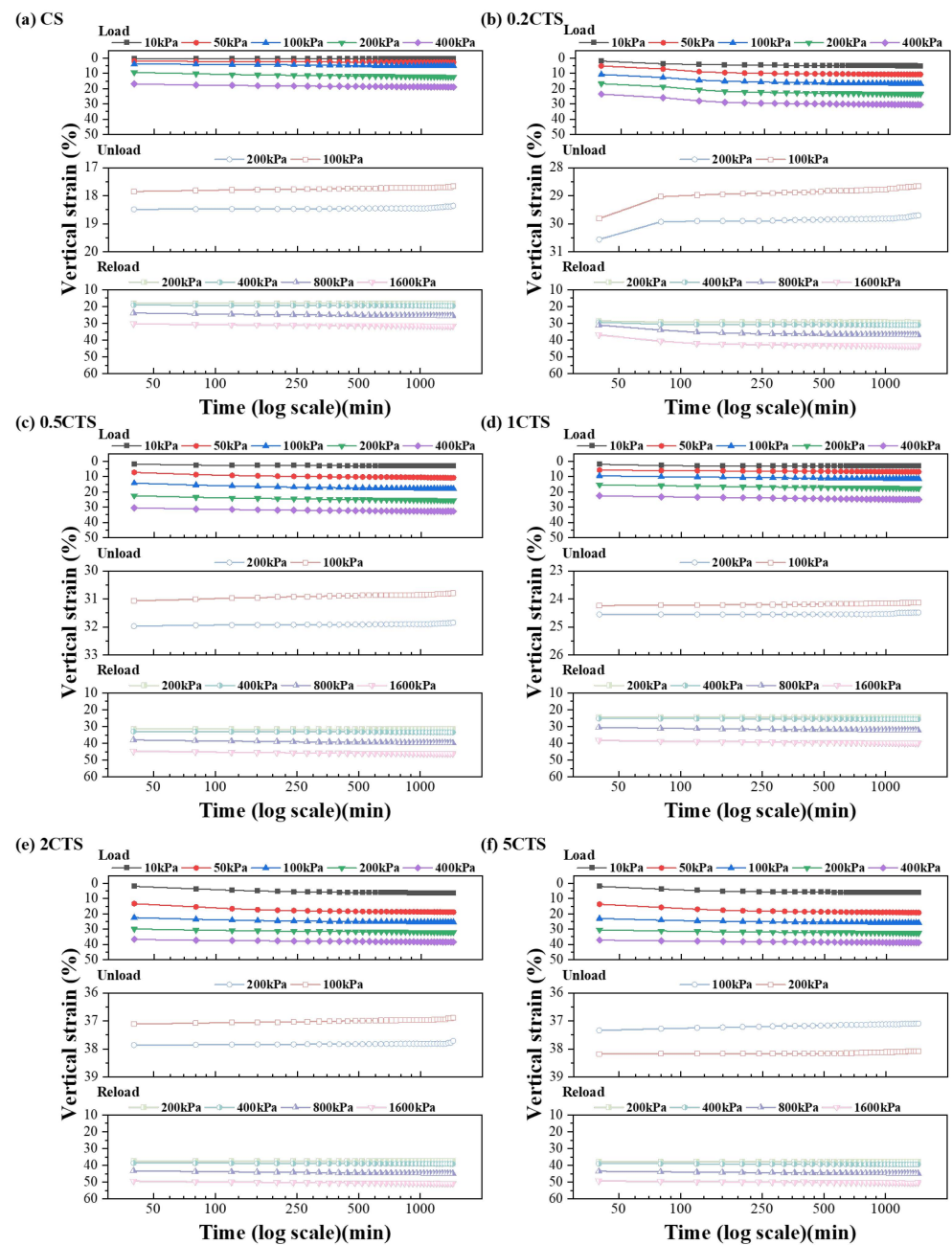
Figure 4. Vertical-strain variation with log scale of time of the samples: (**a**) CS, (**b**) 0.2 CTS, (**c**) 0.5 CTS (**d**) 1 CTS, (**e**) 2 CTS, and (**f**) 5 CTS.

A significant decrease in deformation during the loading and unloading processes was observed and could be attributed to the disruption of the structure connecting soil particles and isomorphic substitution. The addition of a small amount of nZVI (0.2%) converted part of the heavy metal ions into hydroxide/iron oxide precipitates. However, the unstable weak chemical-bond structure failed to impede soil rebound during the unloading process. When the amount of nZVI was increased to 0.5%, more low-intensity heavy metal hydroxide adhered to the soil particle surfaces. The thickness of the diffuse double layer on the soil surface increased, making it more difficult for particles to rebound under external forces due to the formation of a cohesive structure. After treatment with more than 1% nZVI, more nZVI particles could migrate with the pore water, degrading more heavy metal ions as the loading time extends. This gradually led to the formation of larger aggregates composed of iron oxides, hydroxides, and soil particles. As a result, the contact between soil particles

became stronger, further reducing compression and rebound. Under excess conditions (i.e., 2% and 5%), heavy metal ions in the soil were essentially degraded, resulting in the aggregation of nZVI into larger particles, thereby strengthening the connections between particles. In conclusion, it was reported that the disruptive effect of heavy metal ions on the intrinsic bonding structure of soil was observed, which leads to the weakening of interparticle bonds [52–54]. A notable aspect was the varied effects seen in soils treated with different concentrations of nZVI. The influence of nZVI transformed the nature of particle–aggregate connections. At lower dosages, a tendency to establish weaker chemical-bond structures has been noted, whereas, at higher dosages, the formation of more robust physical-bond structures is observed, as proven in [55,56].

In addition, further exploration of the consolidation behavior of the soil is deemed necessary, including the analysis of the soil's creep ratio, consolidation coefficient, and permeability. Figure 5 illustrates the ratio of the creep coefficient to the consolidation coefficient under different consolidation loads, serving as an indicator of soil-deformation behavior. The creep ratio, calculated as the ratio of the creep coefficient (C_α) to the consolidation coefficient (C_v), serves as a measure of the soil's deformation behavior, while the permeability coefficient is used to assess the connectivity of pores within the soil.
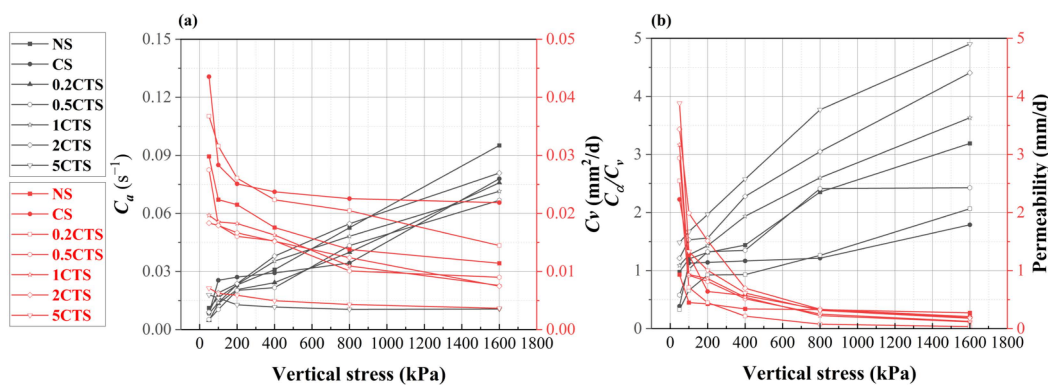
Figure 5. The creep coefficient, consolidation coefficient, and permeability of samples under various consolidation loads: (**a**) C_α and C_v, (**b**) C_α/C_v, and permeability.

The results clearly indicated that soil-deformation behavior and permeability were significantly positively influenced by nZVI. In particular, with an increase in vertical stress, the soil tended to experience rapid settlement while permeability gradually diminished and the creep coefficient of the soil exhibited an overall increasing trend. The consolidation coefficient tended to decrease. Simultaneously, soil permeability demonstrated a positive correlation with the nZVI dosage. The introduction of heavy metal ions resulted in an increase in the consolidation coefficient, while there was a decrease in the creep coefficient under loads exceeding 100 kPa (preconsolidation stress/OCR). This was accompanied by an enhancement in soil permeability. However, for CS, the creep ratio experiences a decrease compared to NS. The introduction of heavy metal ions reduced the soil's Atterberg limits, leading to a decrease in water-retention capacity. Consequently, pore fluids dissipated more quickly, resulting in rapid consolidation, which was characterized by a smaller creep ratio and higher permeability compared to NS.

The addition of a small quantity of nZVI (0.2% and 0.5%) to CS led to fluctuations in the creep coefficient within a range of 0.04, while the consolidation coefficient began to decrease. The creep ratio and permeability of 0.2 CTS and 0.5 CTS started to increase in comparison to CS, and the permeability of CTS increased with the nZVI dosage increasing under the lower stress. With an increase in the dosage of nZVI, the creep coefficient and creep ratio continued to rise while the consolidation coefficient decreased under the same level of loading for treated soil. It was noteworthy that there was not a significant difference in permeability between 800 kPa and 1600 kPa soils. An increase in vertical effective stress resulted in the compression of pore structure, reducing the time required for primary

consolidation and, in turn, accelerating consolidation while reducing permeability. The introduction of a small amount of nZVI introduced relatively fewer but larger particles into the soil, transforming its structure from a destructive arrangement to a weaker chemical-bond structure. Therefore, despite the hindrance posed by small particles to the pore structure, the soil often underwent relatively stable secondary consolidation. With the introduction of 1% or more nZVI, the soil structure was further strengthened, and large aggregates exhibited excellent connectivity, significantly enhancing soil permeability. In the most popular nZVI application of soil remediation, PRB, the combination of a Permeable Reaction Wall (PRB) with nZVI resulted in reduced permeability due to local accumulation from short-distance nanoparticle migration, causing a blocking effect [38,57]. In contrast, the modified slurry consolidation method for in situ treatment of contaminated soil has been found to be beneficial. It resulted in a more uniform distribution of nZVI particles within the soil, facilitating particle migration and thereby enhancing soil permeability. This improvement is notably evidenced by an increase in the permeability (calculated *k* value). These findings underscore the substantial impact of heavy metals and different levels of nZVI on soil-deformation behavior and permeability, reflecting the complex interplay of multiple factors.

The improvement in permeability and deformation paves the way for diverse future applications, be it in construction, agriculture, or ecological restoration. To gain a clearer insight into variations in both the hydraulic and deformation behavior of samples, it is vitally important to consider a multitude of influencing factors. Among these factors, significant impacts are exerted by changes such as Atterberg limits and particle-size distribution [58,59]. In-depth analysis across multiple scales is indispensable for offering a more comprehensive explication of the alterations in the deformation characteristics of the soil.

3.3. Microscopic Characteristics of Soil

3.3.1. Plasticity of Soil Samples

The Atterberg limits (i.e., LL, PL, and PI) are pivotal properties governing a soil's water-retention capacity, compressibility, and plasticity resulting from the presence of bound/free water and its skeleton [60]. The extent of water-bound layers within the soil particle dispersion's double layer was pivotal in determining these characteristics. These bound layers were distinguished as the adsorbed layer and the diffuse layer. This variation in the double-layer thickness could alter the soil's behavior, impacting its ability to retain water, resist deformation, and maintain skeleton structure under varying environmental conditions. Figure 6 illustrates the variations in Atterberg limits across soil types.

With the introduction of nZVI, the PI of nZVI-treated soil exhibited a pattern of initial augmentation succeeded by a decrease (Figure 6). Specifically, the LL experienced an initial increase followed by stabilization with an increase in the nZVI dosage, while the PL displayed an initial increase, followed by a subsequent decrease, and ultimately increasing slightly. Specifically, following contamination, the contaminated soil (CS) was observed to have a reduction in the LL, from 97.0% to 65.0%, a decrease in PL from 62.0% to 52.6%, and a decline in PI from 35.0 to 12.4. As the effect of contaminants cations, Pb(II), Ni(II), and Zn(II) into NS, reactions such as adsorption and occupation of negatively charged binding sites with soil particles and cation concentrations within the pore fluid could lead to a thinning of the soil double layer and less adsorbed water. The phenomenon at the macroscopic level was evident in the reduction of the liquid limit.

Upon the addition of 0.2% nZVI to CS, the LL, PL, and PI increased to 74.2%, 55.4%, and 18.8%, respectively. At a 0.5% nZVI dosage, these values further changed to 87.1%, 64.5%, and 22.6%. Nevertheless, under a 1% nZVI dosage, the PL declined to 60%, while the PI continued to 28.3. With the nZVI dosage reaching 2% and 5%, the LL kept a constant value, while the PL exhibited a minor increase to 62.2% and 67.1%. Hence, it should be noted that the excess nZVI resulted in a continued reduction in the PI, up to 20.51. Upon the introduction of lower concentrations of nZVI (0.2% and 0.5%) into CS, as detailed in the immobilization analysis, a substantial portion of heavy metal contaminants adsorbed

on the soil particle surfaces or present in the pore fluid are promptly transmuted into stable hydroxides (over 72%). This led to the recuperation of the diffusion double-layer thick-ness of some particles. Additionally, the formation of insoluble hydroxides or iron oxide aggregates enhanced the water-retaining capacity of the soil, thereby resulting in an increase in LL, PL, and PI of the treated soil (TS). However, when the nZVI dosage reaches 1%, the 4d degradation efficacy of heavy metal ions was relatively consistent with that of 0.2% and 0.5% (i.e., differences less than 5%). Nevertheless, with the introduction of an increased quantity of nZVI, there was a propensity for the formation of aggregated precipitates within the soil pores. This could adsorb small particles and aggregate larger particles within the soil, causing the liquid limit to remain while the PL increases.
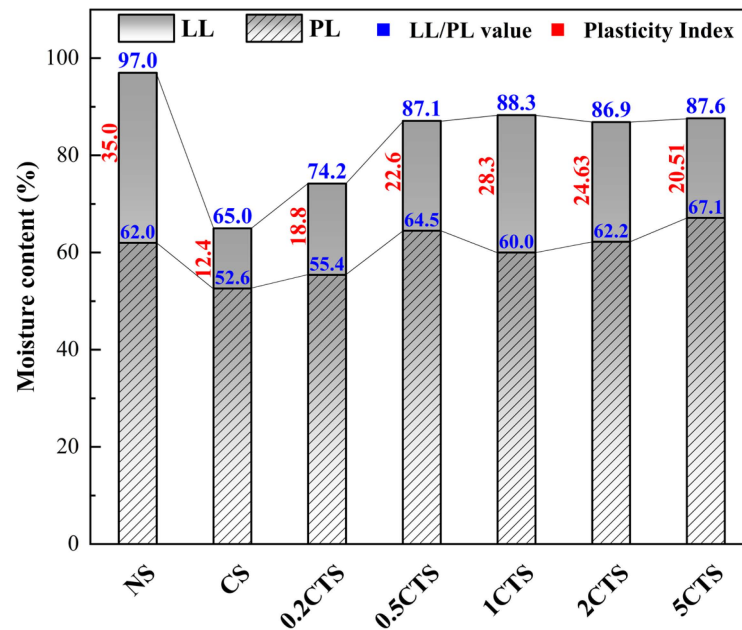

Figure 6. Plasticity—Atterberg limits of each sample.

With the nZVI dosage of 2% and even 5%, the majority of heavy metal ions (over 90%) were expeditiously converted into comparatively stable, nontoxic forms that were adsorbed onto the surfaces of iron oxide aggregates. The cation concentration within the pore fluid significantly diminished, and larger aggregate particles were engendered. Commonly, for a specific type of soil, an increase in soil particle size tends to result in a decrease in the liquid limit, indicating a reduced ability to retain adsorbed water. This observation aligns with the subsequent analysis of particle-size distribution. The mechanism could be rooted in soil particle arrangement, variations in double-layer thickness, degradation of heavy metal ions, and the formation of reaction products. These findings proposed invaluable insights into the comprehension of soil microbehavior and environmental remediation.

The relationship between the Atterberg limits of soil and its consolidation behavior was profound, as the former serves as an indicator of the soil's plasticity and deformability. Specifically, a soil's plasticity and deformability can be inferred from its liquid limits. Soils with higher liquid limits tended to exhibit greater plasticity and deformability, while those with lower liquid limits showed reduced plasticity and deformability. Consequently, the latter soils tended to undergo faster consolidation and demonstrate reduced settlement when subjected to equivalent stress. Moreover, the changes in the plasticity index allowed for macroscopic inferences about the impact of heavy metal ions and nZVI on the microstructure of the soil. Postcontamination, heavy metal ions induced greater dispersion of soil particles, leading to the disruption of the original soil structure. This results in an increase in smaller particles, consequently diminishing cohesion and causing a reduction in the plasticity index. The introduction of nZVI facilitated the degradation of heavy metal

ions, promoting particle aggregation, an increase in the proportion of larger particles, and enhanced interparticle connectivity. The soil experiences a decline in plasticity due to the presence of heavy metal ions, leading to a deterioration in its deformation behavior. On the contrary, the introduction of nZVI heightens the soil's plasticity, reinforcing its resistance to deformation, and ultimately improving its deformation behavior [61,62].

3.3.2. Particle-Size Distribution

The distribution of soil particle sizes is closely related to both the Atterberg limit and the deformation behavior of soils. The objective was to evaluate how changes in soil particle-size distribution led to variations in the deformation and permeability behavior. The summarized PSD results are presented in Figure 7.
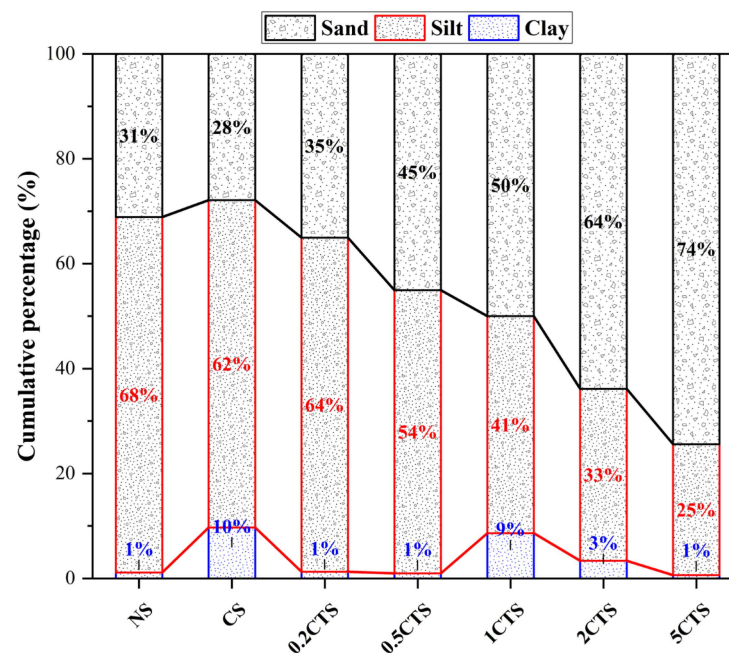

Figure 7. Particle-size distribution of samples after the slurry consolidation process.

It demonstrated a noticeable relationship between the introduction of the nZVI dosage and the increase in soil particle-size distribution. When heavy metal ions were introduced, the soil particle size tended to shift towards smaller particles. To be specific, the proportion of clay in CS increased from 1.1% to 9.7%, while the sand proportion decreased from 31.1% to 27.9 % compared to the NS. After the addition of 0.2% nZVI, the sand proportion significantly raised to 35.1%, while the clay content recovered to that of NS, and the silt proportion stabilized in the range of 62% to 67%. With 0.5% nZVI, the proportions of clay and silt decreased further to 0.97% and 54.0%, respectively, and the sand proportion increased by 10%. When the nZVI dosage reached 1%, the clay content increased significantly to 8.63%, Silt continued to decrease to 41.4%, and sand slightly increased to 50.0%. Continuing to add nZVI up to 2%, the silt's proportion steadily decreased to 32.8%, and sand significantly increased to 63.9%, accompanied by clay decreasing to 3.4%. When the nZVI dosage reached 5%, the proportions of clay and silt decreased to their lowest values of 0.62% and 25.0%, while the sand content reached 74.4%. As previously mentioned, the introduction of heavy metal ions resulted in an increase in the concentration of cations in the pore fluid, weakening the connections between particles and leading to more fractured particles and agglomerates, causing a sharp increase in clay content. However, a small amount of nZVI (0.2% and 0.5%) partially degraded part of heavy metal ions. These ions, along with the nZVI particles, precipitated on the surfaces of soil particles, gradually leading to an increase in particle size. In the 1% dosage scenario, more heavy metal ions were degraded, adsorbed, and precipitated to form larger aggregates of particles. Simultaneously, the lack of nZVI

quantity was insufficient to form larger particles through aggregation and other physical effects, resulting in the phenomenon of increased clay content at the 1% treatment. With an excess input of nZVI (2% and 5%), nonchemical reacted nZVI particles tended to aggregate into larger particles due to their strong magnetic, charge force, and adsorption properties. As a result, the sand proportion continued to increase, while the clay proportion gradually decreased in the 2% and 5%. The particle-size distribution curve results indicate that heavy metal ions disrupt the structure of NS, leading to an increase in the proportion of fine particles. Meanwhile, nZVI, through mechanisms such as heavy metal ion degradation and aggregation, drives CS toward a particle-size distribution dominated by larger particles.

After soil contamination, an increase in the proportion of fine particles leads to a denser soil structure, causing soil particles to form a water film and consequently contribute to easier rearrangement. Hence, the compression of soil in contaminated soil (CS) had a tendency towards rapid settlement. The introduction of nZVI into CS resulted in an increasing proportion of larger particles with the rising dosage. This enhances the soil's microstructures, prompting a higher moisture content to maintain plasticity. Furthermore, the greater strength of the larger aggregates in the nZVI-treated soil skeleton makes it more resistant to compression and swell. Under the same load, the treated soil (TS) tends to exhibit stable secondary consolidation. The PSD results affirmed the earlier speculation that heavy metal ions lead to an increased proportion of finer soil particles, where the soil framework was dominated by small clay particles or agglomerates, resulting in weak deformation behavior and plastic characteristics. Following the treatment of nZVI, the proportion of larger particles was positively correlated with its dosage. While efficiently immobilizing contaminants, the increased presence of larger particles contributes to a denser soil skeleton, thereby enhancing compressibility and plasticity [63].

4. Conclusions

The objective of this study is to investigate the influence of nano zero-valent iron (nZVI) on the deformation behavior of combined heavy metal (Pb(II), Ni(II), and Zn(II)) contaminated soil through the modified slurry consolidation method. A macro–micro experiment program including the Oedometer tests, and a series of microscopic characterization experiments (cone penetrometer method and PSD) were conducted. The conclusions drawn from the aforementioned results and discussion are as follows.

(a) nZVI efficiently degraded the combined heavy metal ions in the soil, with degradation efficiency exceeding 90% at 2% nZVI after 4 days of a slurry consolidation process. The efficiency showed a positive correlation with a higher nZVI dosage, showing 98%—Pb(II), 85%—Zn(II), and 75% Ni(II) at 1% nZVI. All three heavy metal ions were degraded, exceeding 98% at 5%;

(b) Post-nZVI treatment has a positive effect on soil deformation and permeability by the slurry consolidation process, such as lower soil compressibility, swelling index, and increasing permeability. With rising nZVI dosages, the creep ratio and permeability increased due to the shift from weakened chemical bonds to strengthened physical aggregation structures with the formation of larger aggregates. The presence of three heavy metal ions weakened soil resistance, increased the compression index, decreased the swelling index, and reduced the creep ratio. This was attributed to the weakened interparticle connections, higher clay content, and thinner diffusion layers, allowing easier particle slippage;

(c) The Atterberg limits of nZVI-treated soil raised with nZVI dosages due to the degradation of heavy metal ions and improved plasticity and water retention from the formation of insoluble hydroxides or iron oxide aggregate with soil particles. After contamination with the combined heavy metal ions in the soil, the Atterberg limits decreased due to higher cation concentration in pore fluid, occupying soil particle binding sites, and thinning the diffuse double layer;

(d) The proportion of clay particles dramatically increased in CS, confirming the earlier increase in fragmented particles. In TS, as the nZVI dosage increases, the sand

proportion of soil particles gradually rises, especially at 2% and 5%. It should be summarized that unreacted nZVI particles tended to aggregate for larger particles due to their strong magnetism, adsorption, and aggregation, thus stabilizing their chemical effects.

This study represents an indicative investigation into the deformation characteristics and microstructure of combined heavy metal-contaminated soil treated by nZVI. nZVI demonstrated excellent efficiency in degrading combined heavy metal ions in soil and concurrently enhanced its deformation properties and permeability. Our research illustrated the potential of applying nanotechnology within geotechnical engineering for environmental sustainability. This approach could transform our methods of addressing environmental challenges, providing more efficient, safe, and sustainable solutions. We believe that this research could be an indicator for future nanomaterials research in soil, contributing to the sustainable research development of Nano-Geotechnical Engineering. However, further sustainable research is recommended concerning the on-site application and optimization of nZVI for remediating combined contaminants in soil and long-term safety.

Institutional Review Board Statement: Not applicable.

Informed Consent Statement: Not applicable.

Data Availability Statement: The data presented in this study are available on request from the corresponding author.

Conflicts of Interest: The authors declare no conflict of interest.

References

1. Wall, D.H.; Nielsen, U.N.; Six, J. Soil biodiversity and human health. *Nature* **2015**, *528*, 69–76. [CrossRef] [PubMed]
2. Guerra, C.A.; Bardgett, R.D.; Caon, L.; Crowther, T.W.; Delgado-Baquerizo, M.; Montanarella, L. Tracking, targeting, and conserving soil biodiversity. *Science* **2021**, *371*, 239–241. [CrossRef]
3. Liao, J.; Wen, Z.; Ru, X.; Chen, J.; Wu, H.; Wei, C. Distribution and migration of heavy metals in soil and crops affected by acid mine drainage: Public health implications in Guangdong Province, China. *Ecotoxicol. Environ. Saf.* **2016**, *124*, 460–469. [CrossRef] [PubMed]
4. Huang, B.; Yuan, Z.; Li, D.; Zheng, M.; Nie, X.; Liao, Y. Effects of soil particle size on the adsorption, distribution, and migration behaviors of heavy metal (loid) s in soil: A review. *Environ. Sci. Process. Impacts* **2020**, *22*, 1596–1615. [CrossRef] [PubMed]
5. Huang, J.; Guo, S.; Zeng, G.; Li, F.; Gu, Y.; Shi, Y.; Shi, L.; Liu, W.; Peng, S. A new exploration of health risk assessment quantification from sources of soil heavy metals under different land use. *Environ. Pollut.* **2018**, *243*, 49–58. [CrossRef] [PubMed]
6. World's Worst Pollution Problems. *The New Top Six Toxic Threats: A Priority List for Remediation*; Pure Earth: Zurich, Switzerland, 2016.
7. Alengebawy, A.; Abdelkhalek, S.T.; Qureshi, S.R.; Wang, M.Q. Heavy metals and pesticides toxicity in agricultural soil and plants: Ecological risks and human health implications. *Toxics* **2021**, *9*, 42. [CrossRef]
8. Grandjean, P.; Landrigan, P.J. Neurobehavioural effects of developmental toxicity. *Lancet Neurol.* **2014**, *13*, 330–338. [CrossRef]
9. Song, W.E.; Chen, S.B.; Liu, J.F.; Chen, L.; Song, N.N.; Li, N.; Liu, B. Variation of Cd concentration in various rice cultivars and derivation of cadmium toxicity thresholds for paddy soil by species-sensitivity distribution. *J. Integr. Agric.* **2015**, *14*, 1845–1854. [CrossRef]
10. Mohammadi, A.; Mansour, S.N.; Najafi, M.L.; Toolabi, A.; Abdolahnejad, A.; Faraji, M.; Miri, M. Probabilistic risk assessment of soil contamination related to agricultural and industrial activities. *Environ. Res.* **2022**, *203*, 111837. [CrossRef]
11. Sabet Aghlidi, P.; Cheraghi, M.; Lorestani, B.; Sobhanardakani, S.; Merrikhpour, H. Analysis, spatial distribution and ecological risk assessment of arsenic and some heavy metals of agricultural soils, case study: South of Iran. *J. Environ. Health Sci. Eng.* **2020**, *18*, 665–676. [CrossRef]
12. European Environment Agency. *Air Quality in Europe—2018 Report*; European Environment Agency: Copenhagen, Denmark, 2018.

13. EPA US. *Cleaning up the Nation's Waste Sites: Markets and Technology Trends*; National Technical Information; United States Environmental Protection Agency: Washington, DC, USA, 2004.

14. The Ministry of Environmental Protection (MEP). *The Ministry of Land and Resources Report on the National Soil Contamination Survey*; Ministry of Environmental Protection of the People's Republic of China: Beijing, China, 2014.

15. Xi, Y.; Mallavarapu, M.; Naidu, R. Reduction and adsorption of Pb^{2+} in aqueous solution by nano-zero-valent iron—A SEM, TEM and XPS study. *Mater. Res. Bull.* **2010**, *45*, 1361–1367. [CrossRef]

16. Efecan, N.; Shahwan, T.; Eroğlu, A.E.; Lieberwirth, I. Characterization of the uptake of aqueous Ni^{2+} ions on nanoparticles of zero-valent iron (nZVI). *Desalination* **2009**, *249*, 1048–1054. [CrossRef]

17. Rathor, G.; Chopra, N.; Adhikari, T. Remediation of nickel ion from soil and water using Nano particles of zero-valent Iron (nZVI). *Orient. J. Chem.* **2016**, *33*, 1025. [CrossRef]

18. Gil-Díaz, M.; Ortiz, L.T.; Costa, G.; Alonso, J.; Rodríguez-Membibre, M.L.; Sánchez-Fortún, S. Immobilization and leaching of Pb and Zn in an acidic soil treated with zerovalent iron nanoparticles (nZVI): Physicochemical and toxicological analysis of leachates. *Water Air Soil Pollut.* **2014**, *225*, 1990. [CrossRef]

19. Vasarevičius, S.; Danila, V.; Januševičius, T. Immobilisation of cadmium, copper, lead, and nickel in soil using nano zerovalent iron particles: Ageing effect on heavy metal retention. *Water Air Soil Pollut.* **2020**, *231*, 496. [CrossRef]

20. He, M.; Shi, H.; Zhao, X.; Yu, Y.; Qu, B. Immobilization of Pb and Cd in contaminated soil using nano-crystallite hydroxyapatite. *Procedia Environ. Sci.* **2013**, *18*, 657–665. [CrossRef]

21. Arabyarmohammadi, H.; Darban, A.K.; Abdollahy, M.; Yong, R.; Ayati, B.; Zirakjou, A.; Van der Zee, S.E. Utilization of a novel chitosan/clay/biochar nanobiocomposite for immobilization of heavy metals in acid soil environment. *J. Polym. Environ.* **2018**, *26*, 2107–2119. [CrossRef]

22. Lian, M.; Wang, L.; Feng, Q.; Niu, L.; Zhao, Z.; Wang, P.; Song, C.; Li, X.; Zhang, Z. Thiol-functionalized nano-silica for in-situ remediation of Pb, Cd, Cu contaminated soils and improving soil environment. *Environ. Pollut.* **2021**, *280*, 116879. [CrossRef]

23. Mohammed, S.A.S.; Sanaulla, P.F.; Alnuaim, A.M.; Moghal, A.A.B. Role of Different Leaching Methods to Arrest the Transport of Ni^{2+} in Soil and Soil Amended with Nano Calcium Silicate. *Geo-China* **2016**, *2016*, 49–56.

24. Wang, J.; Liu, G.; Li, T.; Zhou, C.; Qi, C. Zero-valent iron nanoparticles (NZVI) supported by kaolinite for CuII and NiII ion removal by adsorption: Kinetics, thermodynamics, and mechanism. *Aust. J. Chem.* **2015**, *68*, 1305–1315. [CrossRef]

25. Sang, L.; Wang, G.; Liu, L.; Bian, H.; Jiang, L.; Wang, H.; Zhang, Y.; Zhang, W.; Peng, C.; Wang, X. Immobilization of Ni (II) at three levels of contaminated soil by rhamnolipids modified nano zero valent iron (RL@ nZVI): Effects and mechanisms. *Chemosphere* **2021**, *276*, 130139. [CrossRef] [PubMed]

26. Karabelli, D.; Üzüm, C.; Shahwan, T.; Eroglu, A.E.; Scott, T.B.; Hallam, K.R.; Lieberwirth, I. Batch removal of aqueous Cu^{2+} ions using nanoparticles of zero-valent iron: A study of the capacity and mechanism of uptake. *Ind. Eng. Chem. Res.* **2008**, *47*, 4758–4764. [CrossRef]

27. Zhang, Y.; Su, Y.; Zhou, X.; Dai, C.; Keller, A.A. A new insight on the core–shell structure of zerovalent iron nanoparticles and its application for Pb (II) sequestration. *J. Hazard. Mater.* **2013**, *263*, 685–693. [CrossRef] [PubMed]

28. Tang, S.C.N.; Lo, I.M.C. Magnetic nanoparticles: Essential factors for sustainable environmental applications. *Water Res.* **2013**, *47*, 2613–2632. [CrossRef] [PubMed]

29. Adusei-Gyamfi, J.; Acha, V. Carriers for nano zerovalent iron (nZVI): Synthesis, application and efficiency. *RSC Adv.* **2016**, *6*, 91025–91044. [CrossRef]

30. Lu, H.J.; Wang, J.K.; Ferguson, S.; Wang, T.; Bao, Y.; Hao, H. Mechanism, synthesis and modification of nano zerovalent iron in water treatment. *Nanoscale* **2016**, *8*, 9962–9975. [CrossRef] [PubMed]

31. Chen, Y.Z.; Zhou, W.H.; Liu, F.; Yi, S. Exploring the effects of nanoscale zero-valent iron (nZVI) on the mechanical properties of lead-contaminated clay. *Can. Geotech. J.* **2019**, *56*, 1395–1405. [CrossRef]

32. Yang, Z.; Elgamal, A. Influence of permeability on liquefaction-induced shear deformation. *J. Eng. Mech.* **2002**, *128*, 720–729. [CrossRef]

33. Eggers, C.G.; Berli, M.; Accorsi, M.L.; Or, D. Deformation and permeability of aggregated soft earth materials. *J. Geophys. Res. Solid Earth* **2006**, *111*, B10204. [CrossRef]

34. Sadiq, A.S.; Fattah, M.Y.; Aswad, M.F. Enhancement of Clay Compressibility and Strength Using Nano Magnesium Oxide. *E3S Web Conf.* **2023**, *427*, 01013. [CrossRef]

35. Luo, X.; Kong, L.; Bai, W. Effect of Superhydrophobic Nano-SiO2 on the Hydraulic Conductivity of Expansive Soil and Analysis of Its Mechanism. *Appl. Sci.* **2023**, *13*, 8198. [CrossRef]

36. Ouhadi, V.R.; Noori, A. Impact of Nano-Clay on Consolidation and Permeability Behaviour of Bentonite in the Presence of Heavy Metal Contaminant. *Modares Civ. Eng. J.* **2013**, *13*, 1–10.

37. Chen, Y.Z.; Zhou, W.H.; Liu, F.; Yi, S.; Geng, X. Microstructure and morphological characterization of lead-contaminated clay with nanoscale zero-valent iron (nZVI) treatment. *Eng. Geol.* **2019**, *256*, 84–92. [CrossRef]

38. Antia, D.D.J. Hydrodynamic Decontamination of Groundwater and Soils Using ZVI. *Water* **2023**, *15*, 540. [CrossRef]

39. Li, Y.; Zhao, H.P.; Zhu, L. Remediation of soil contaminated with organic compounds by nanoscale zero-valent iron: A review. *Sci. Total Environ.* **2021**, *760*, 143413. [CrossRef]

40. *ASTM D4318-17*; Standard Test Method for Liquid Limit, Plastic Limit, and Plasticity Index of Soils. ASTM International: West Conshohocken, PA, USA, 2017.

41. *ASTM D698-12*; Standard Test Method for Laboratory Compaction Characteristics of Soil Using Standard Effort (12400 ft-lbf/ft3 (600 kN-m/m3)). ASTM International: West Conshohocken, PA, USA, 2021.

42. *ASTM D2487-17*; Standard Test Method for Classification of Soils for Engineering Purposes (Unified Soil Classification System). ASTM International: West Conshohocken, PA, USA, 2017.

43. Huang, P.; Ye, Z.; Xie, W.; Chen, Q.; Li, J.; Xu, Z.; Yao, M. Rapid magnetic removal of aqueous heavy metals and their relevant mechanisms using nanoscale zero valent iron (nZVI) particles. *Water Res.* **2013**, *47*, 4050–4058. [CrossRef]

44. Li, S.; Wang, W.; Liang, F.; Zhang, W.X. Heavy metal removal using nanoscale zero-valent iron (nZVI): Theory and application. *J. Hazard. Mater.* **2017**, *322*, 163–171. [CrossRef]

45. *ASTM D2435/D2435M−11*; Standard Test Method for One-Dimensional Consolidation Properties of Soils Using Incremental Loading. ASTM International: West Conshohocken, PA, USA, 2020.

46. U.S. Environmental Protection Agency. *Test Methods for Evaluating Solid Waste (SW-846)*; U.S. Environmental Protection Agency: Washington, DC, USA, 2015.

47. Liang, Z.; Peng, X.; Luan, Z. Immobilization of Cd, Zn and Pb in sewage sludge using red mud. *Environ. Earth Sci.* **2012**, *66*, 1321–1328. [CrossRef]

48. Zhao, L.; Cao, X.; Zheng, W. Copyrolysis of biomass with phosphate fertilizers to improve biochar carbon retention, slow nutrient release, and stabilize heavy metals in soil. *ACS Sustain. Chem. Eng.* **2016**, *4*, 1630–1636. [CrossRef]

49. Diao, Z.H.; Du, J.J.; Jiang, D.; Kong, L.J.; Huo, W.Y.; Liu, C.M.; Wu, Q.H.; Xu, X.R. Insights into the simultaneous removal of Cr^{6+} and Pb^{2+} by a novel sewage sludge-derived biochar immobilized nanoscale zero valent iron: Coexistence effect and mechanism. *Sci. Total Environ.* **2018**, *642*, 505–515. [CrossRef]

50. Kržišnik, N.; Mladenovič, A.; Škapin, A.S.; Škrlep, L.; Ščančar, J.; Milačič, R. Nanoscale zero-valent iron for the removal of Zn^{2+}, Zn(II)–EDTA and Zn(II)–citrate from aqueous solutions. *Sci. Total Environ.* **2014**, *476*, 20–28. [CrossRef] [PubMed]

51. Apriliani, N. Green Synthesis of Nanoscale Zero-Valent Iron and Its Activity as an Adsorbent for Ni(II) and Cr(VI). *Chem. Mater.* **2022**, *1*, 71–76. [CrossRef]

52. Fan, R.D.; Liu, S.Y.; Du, Y.J.; Reddy, K.R.; Yang, Y.L. Impacts of presence of lead contamination on settling behavior and microstructure of clayey soil-calcium bentonite blends. *Appl. Clay Sci.* **2017**, *142*, 109–119. [CrossRef]

53. Caporale, A.G.; Violante, A. Chemical processes affecting the mobility of heavy metals and metalloids in soil environments. *Curr. Pollut. Rep.* **2016**, *2*, 15–27. [CrossRef]

54. Li, Q.; Wang, Y.; Li, Y.; Li, L.; Tang, M.; Hu, W.; Chen, L.; Ai, S. Speciation of heavy metals in soils and their immobilization at micro-scale interfaces among diverse soil components. *Sci. Total Environ.* **2022**, *825*, 153862. [CrossRef] [PubMed]

55. Wu, W.; Chen, X.; Han, L.; Yang, L.; Gu, M.; Li, J.; Chen, M. The evolution of stable nanohybrids to complex heteroaggregates between nZVI and soil nanoparticles: The influence of ionic strength and soil components. *J. Hazard. Mater.* **2022**, *436*, 129155. [CrossRef] [PubMed]

56. Van Koetsem, F.; Van Havere, L.; Du Laing, G. Impact of carboxymethyl cellulose coating on iron sulphide nanoparticles stability, transport, and mobilization potential of trace metals present in soils and sediment. *J. Environ. Manag.* **2016**, *168*, 210–218. [CrossRef] [PubMed]

57. Singh, R.; Chakma, S.; Birke, V. Performance of field-scale permeable reactive barriers: An overview on potentials and possible implications for in-situ groundwater remediation applications. *Sci. Total Environ.* **2023**, *858*, 158838. [CrossRef]

58. Zekkos, D.; Kabalan, M.; Syal, S.M.; Hambright, M.; Sahadewa, A. Geotechnical characterization of a municipal solid waste incineration ash from a Michigan monofil. *Waste Manag.* **2013**, *33*, 1442–1450. [CrossRef]

59. Polidori, E. Relationship between the Atterberg limits and clay content. *Soils Found.* **2007**, *47*, 887–896. [CrossRef]

60. Zhou, B.; Lu, N. Correlation between Atterberg limits and soil adsorptive water. *J. Geotech. Geoenviron. Eng.* **2021**, *147*, 04020162. [CrossRef]

61. Moghal, A.A.B.; Ashfaq, M.; Al-Shamrani, M.A.; Al-Mahbashi, A. Effect of heavy metal contamination on the compressibility and strength characteristics of chemically modified semiarid soils. *J. Hazard. Toxic Radioact. Waste* **2020**, *24*, 04020029. [CrossRef]

62. Mar Gil-Díaz, M.; Pérez-Sanz, A.; Angeles Vicente, M.; Carmen Lobo, M. Immobilisation of Pb and Zn in soils using stabilised zero-valent iron nanoparticles: Effects on soil properties. *Clean–Soil Air Water* **2014**, *42*, 1776–1784. [CrossRef]

63. Li, J.S.; Xue, Q.; Wang, P.; Li, Z.Z. Effect of lead (II) on the mechanical behavior and microstructure development of a Chinese clay. *Appl. Clay Sci.* **2015**, *105*, 192–199. [CrossRef]